

CONTRIBUTION FROM THE DEPARTMENT OF CHEMISTRY,
UNIVERSITY OF CONNECTICUT, STORRS, CONNECTICUT

The Modification of Structures of Ternary Oxides by Cation Substitution. I. Substitution of Strontium for Barium in Barium Ruthenium Oxide and in Barium Iridium Oxide

By PAUL C. DONOHUE, LEWIS KATZ, AND ROLAND WARD

Received August 2, 1965

The effect of variation of the depth of close-packed AO_3 layers on the structures of compounds of the type AMO_3 is studied using the systems $\text{Ba}_{1-x}\text{Sr}_x\text{RuO}_3$ and $\text{Ba}_{1-x}\text{Sr}_x\text{IrO}_3$. It is found that with increasing values of x the nine-layer structure with stacking sequence chh gives way to the four-layer structure (ch,ch) and finally to the three-layer perovskite-type structure (c,c,c). With ruthenium, the successive changes occur when x is about $1/6$ and $1/3$. The iridium case is more complex. Barium iridium oxide has a structure which is based on a superlattice of that of the ruthenium compound. It is probably oxygen deficient. The transformations to the four-layer structure and to the perovskite-type structure occur at somewhat higher strontium content. Some barium is necessary to stabilize the perovskite-type phase.

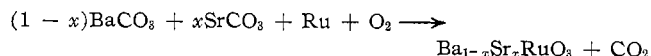
Introduction

A correlation of the structures of a number of ternary oxides containing a large cation A and a smaller cation M can be made on the basis of cubic and hexagonal close packing of layers of composition AO_3 , the M cations occupying the octahedral interstices among the oxide ions.¹ In the case where all of the octahedral sites are occupied, the formula is AMO_3 . Hexagonal close packing leads to face sharing of the oxygen octahedra. It has been suggested that hexagonal close packing is promoted by interactions between adjacent M cations either by direct metal-metal bonds involving d electrons or d orbitals and polarizable anions.^{1,2} It has been observed that, for most of the compounds of this type, the A cation is the largest of its species— Cs^+ or Ba^{2+} ^{1,2}—while smaller A cation analogs are cubic close packed.

The structure of BaRuO_3 has been shown to have the stacking sequence chh. The three face-sharing oxygen octahedra contain ruthenium ions.³ The analogous strontium compound, SrRuO_3 , was characterized as an orthorhombic perovskite-type compound.⁴ The AO_3 stacking sequence in this compound is entirely cubic. It was of some interest to study the effect of A cation substitution on these structures.

Experimental Section

The System $\text{Ba}_{1-x}\text{Sr}_x\text{RuO}_3$. Preparation.—The preparation of phases in the system $\text{Ba}_{1-x}\text{Sr}_x\text{RuO}_3$ was effected by heating appropriate mixtures of barium and strontium carbonates with finely divided elemental ruthenium in air at temperatures from 1000 to 1200°. Repeated regrinding between heat treatments served to give homogeneous products. The stoichiometry is represented by the equation



The carbonates were used in preference to the oxides merely because they are easier to handle. Five values of x from $1/12$ to $2/3$ were used. With $x \geq 1/2$, the products of these reactions gave diffraction patterns corresponding to the orthorhombic perovskite structure only. The product at 1000° from the mixture with composition $x = 1/12$ gave a powder diffraction pattern corresponding to the nine-layer structure of BaRuO_3 with an appreciably smaller unit cell. The product of the same mixture at 1100° gave, in addition, lines of a new phase (X) and, at 1200°, only the pattern of X. It is apparent that the tolerance of the barium ruthenium oxide structure for strontium substitution is quite low. The phase X appeared along with the nine-layer phase at 1000° when $x = 1/6$. At 1100 and 1200° this mixture gave only phase X. At 1000° when $x = 1/3$, phase X appeared along with the perovskite-like phase. It seemed reasonable to suppose that phase X would have a close-packed structure since its composition was intermediate between those of two other close-packed structures. This indeed was found. The pattern corresponding to the composition $\text{Ba}_{5/6}\text{Sr}_{1/6}\text{RuO}_3$ appeared to be entirely due to phase X.

Structure of $\text{Ba}_{5/6}\text{Sr}_{1/6}\text{RuO}_3$.—The powder pattern was indexed on the basis of a hexagonal cell $a = 5.712 \pm 0.005$ Å and $c = 9.488 \pm 0.005$ Å. The a axis is thus of the proper di-

- (1) L. Katz and R. Ward, *Inorg. Chem.*, **3**, 205 (1964).
- (2) G. Blasse, *J. Inorg. Nucl. Chem.*, **27**, 993 (1965).
- (3) P. C. Donohue, L. Katz, and R. Ward, *Inorg. Chem.*, **4**, 306 (1965).
- (4) J. J. Randall and R. Ward, *J. Am. Chem. Soc.*, **81**, 2629 (1959).

mension for the AO_3 layer where A is mostly Ba^{2+} , and the c axis is about 4 times the thickness of such an AO_3 layer. The only structure of this kind so far described is that of the high-temperature form of BaMnO_3 .⁵

Some small single crystals were obtained by the slow cooling from 1100° of a mixture using excess of barium chloride as a flux. The crystals appeared to be cracked, and the spot quality of the precession photographs was rather poor, but sufficient data were obtained to confirm the cell dimensions derived from powder data. The structure determination and refinement were based on powder data.

Intensities were measured by weighing cutout tracings of the powder pattern peaks. Intensities were calculated for the composition $\text{Ba}_{5/6}\text{Sr}_{1/6}\text{RuO}_3$ in space group $\text{P6}_3/\text{mmc}$. The positions used are listed in Table I. Using the ideal parameters $z = 0.875$ for Ru and $x = 5/6$ for O, the R factor based on intensities was 21.3%. With $z = 0.890$ for Ru, the value which corresponds to the separation in BaRuO_3 , the R factor dropped to 16.7%. The four-layer arrangement similar to that of high-temperature BaMnO_3 is thus well established for $\text{Ba}_{5/6}\text{Sr}_{1/6}\text{RuO}_3$. The indexing and intensity data are shown in Table II.

TABLE I

| ATOMIC POSITIONS FOR $\text{Ba}_{5/6}\text{Sr}_{1/6}\text{RuO}_3$ SPACE GROUP $\text{P6}_3/\text{mmc}$ | |
|--|--|
| $2(\text{Ba}_{5/6}\text{Sr}_{1/6})$ | a 0, 0, 0; 0, 0, $1/2$ |
| $2(\text{Ba}_{5/6}\text{Sr}_{1/6})$ | c $1/3, 2/3, 1/4; 2/3, 1/3, 3/4$ |
| 4 Ru | f $1/3, 2/3, z; 2/3, 1/3, \bar{z}; 2/3, 1/3, 1/2 + z; 1/3, 2/3, 1/2 - z$ |
| 6 O | g $1/2, 0, 0; 0, 1/2, 0; 1/2, 1/2, 0; 1/2, 0, 1/2; 0, 1/2, 1/2; 1/2, 1/2, 1/2$ |
| 6 O | h $x, 2x, 1/4; 2\bar{x}, \bar{x}, 1/4; x, \bar{x}, 1/4; \bar{x}, 2\bar{x}, 3/4; 2x, x, 3/4; \bar{x}, x, 3/4$ |

TABLE II

| X-RAY POWDER DATA FOR $\text{Ba}_{5/6}\text{Sr}_{1/6}\text{RuO}_3$ | | | | | | | | | | | | | |
|--|---|---|-------|-------|-------|-------|---|---|---|-------|-------|------|------|
| H | K | L | DOBS | DCAL | IOBS | ICAL | H | K | L | DOBS | DCAL | IOBS | ICAL |
| 1 | 0 | 0 | 4.954 | 4.948 | 7.0 | 5.1 | 3 | 1 | 2 | 1.318 | 1.318 | 5.9 | 5.9 |
| 1 | 0 | 1 | 4.390 | 4.387 | 6.0 | 2.3 | 3 | 1 | 3 | 1.259 | 1.259 | 8.6 | 10.7 |
| 1 | 0 | 2 | 3.430 | 3.423 | 57.4 | 43.8 | 2 | 1 | 6 | 1.207 | 1.207 | 5.5 | 6.6 |
| 1 | 1 | 0 | 2.859 | 2.857 | 100.0 | 104.0 | 4 | 0 | 2 | 1.196 | 1.197 | 2.5 | 3.8 |
| 1 | 0 | 3 | 2.667 | 2.665 | 63.0 | 53.7 | 3 | 1 | 4 | 1.187 | 1.188 | 7.4 | 3.8 |
| 2 | 0 | 1 | 2.392 | 2.394 | .6 | .6 | 0 | 0 | 8 | | 1.186 | | 3.0 |
| 0 | 0 | 4 | 2.370 | 2.372 | 4.0 | 2.3 | 4 | 0 | 3 | 1.151 | 1.152 | 5.0 | 5.1 |
| 2 | 0 | 2 | 2.192 | 2.194 | 35.3 | 32.3 | 3 | 1 | 5 | 1.112 | 1.112 | 4.3 | 5.0 |
| 1 | 0 | 4 | 2.138 | 2.139 | 15.5 | 12.9 | 3 | 2 | 2 | 1.104 | 1.104 | 3.0 | 3.6 |
| 2 | 0 | 3 | 1.949 | 1.949 | 32.1 | 30.2 | 1 | 1 | 8 | 1.095 | 1.095 | 11.3 | 11.2 |
| 2 | 1 | 0 | 1.868 | 1.870 | .7 | .7 | 4 | 1 | 0 | 1.079 | 1.079 | 7.2 | 11.7 |
| 1 | 1 | 4 | 1.826 | 1.825 | .2 | .3 | 3 | 2 | 3 | 1.071 | 1.068 | 4.6 | 6.9 |
| 1 | 0 | 5 | 1.771 | 1.772 | 11.4 | 11.0 | 3 | 1 | 6 | 1.036 | 1.036 | 5.9 | 6.4 |
| 2 | 1 | 2 | 1.739 | 1.740 | 10.8 | 14.8 | 4 | 0 | 5 | | 1.038 | | 1.7 |
| 2 | 0 | 4 | 1.712 | 1.712 | 8.9 | 8.2 | 4 | 0 | 6 | .9741 | .9735 | 4.0 | 3.1 |
| 3 | 0 | 0 | 1.650 | 1.649 | 21.0 | 21.9 | 3 | 2 | 5 | | .9742 | | 3.9 |
| 2 | 1 | 3 | 1.609 | 1.610 | 21.7 | 24.4 | 3 | 0 | 8 | .9627 | .9630 | 7.4 | 9.6 |
| 1 | 0 | 6 | 1.505 | 1.507 | 17.5 | 6.5 | 3 | 0 | 0 | .9519 | .9523 | 3.5 | 5.1 |
| 2 | 0 | 5 | | 1.506 | | 8.3 | 5 | 0 | 3 | .9440 | .9445 | .2 | 3.0 |
| 2 | 1 | 4 | 1.468 | 1.469 | 9.9 | 7.8 | 2 | 3 | 6 | .9217 | .9222 | 2.5 | 4.4 |
| 2 | 2 | 0 | 1.428 | 1.428 | 14.3 | 18.0 | 2 | 2 | 8 | .9122 | .9126 | 12.0 | 13.3 |
| 2 | 0 | 6 | 1.332 | 1.332 | 16.0 | 6.3 | 4 | 2 | 3 | .8961 | .8968 | 4.8 | 7.9 |
| 2 | 1 | 5 | | 1.332 | | 8.3 | | | | | | | |

In order to refine parameters further, the resolved reflections from the powder data were converted to structure factors by taking square roots after dividing out the Lorentz and polarization corrections and the multiplicities. These reflections, 31 in all, were used in the Busing, Martin, and Levy least-squares program.⁶ An over-all temperature factor and the two position parameters were refined. After three cycles the R factor (based on structure factors) dropped to 6.8%. The final parameters were 0.8807 ± 0.0021 for Ru and 0.829 ± 0.012 for O. The observed and calculated structure factors are listed in Table III. Bond distances and angles are shown in Table IV. Figure 1 shows the four-layer structure, with the atoms numbered as in Table IV.

The System $\text{Ba}_{1-x}\text{Sr}_x\text{IrO}_3$. Preparation and X-Ray Analysis.— BaIrO_3 , prepared by the reaction of BaO_2 and Ir metal heated at 1000° in air, was previously reported to have a powder diffraction similar to that of BaRuO_3 .³ The main reflections could

(5) A. Hardy, *Bull. Soc. Chim. France*, 1329 (1961).

(6) W. R. Busing, K. O. Martin, and H. A. Levy, Oak Ridge National Laboratory Report ORNL-TM-305 (1962).

TABLE III
OBSERVED AND CALCULATED FACTORS FOR RESOLVED
POWDER REFLECTIONS OF $\text{Ba}_{5/6}\text{Sr}_{1/6}\text{RuO}_3$

| H | K | L | FOBS | FCAL* | H | K | L | FOBS | FCAL* |
|---|---|---|------|-------|---|---|---|------|-------|
| 1 | 0 | 0 | 12.1 | 10.9 | 2 | 1 | 3 | 37.7 | 39.0 |
| 1 | 0 | 1 | 9.0 | 5.4 | 2 | 1 | 4 | 28.4 | 24.7 |
| 1 | 0 | 2 | 36.0 | 35.2 | 2 | 2 | 0 | 80.5 | 78.8 |
| 1 | 1 | 0 | 82.2 | 89.1 | 3 | 1 | 2 | 24.9 | 25.3 |
| 1 | 0 | 3 | 48.9 | 47.7 | 3 | 1 | 3 | 31.6 | 32.7 |
| 2 | 0 | 1 | 5.5 | 6.7 | 2 | 1 | 6 | 26.4 | 27.3 |
| 0 | 0 | 4 | 35.1 | 30.2 | 4 | 0 | 2 | 25.3 | 30.5 |
| 2 | 0 | 2 | 46.6 | 48.5 | 4 | 0 | 3 | 37.1 | 34.0 |
| 1 | 0 | 4 | 32.2 | 29.5 | 3 | 1 | 5 | 25.0 | 25.1 |
| 2 | 0 | 3 | 51.1 | 51.4 | 3 | 2 | 2 | 20.9 | 22.7 |
| 2 | 1 | 0 | 10.4 | 6.9 | 1 | 1 | 8 | 57.6 | 53.1 |
| 1 | 1 | 4 | 10.7 | 6.5 | 4 | 1 | 0 | 53.5 | 53.4 |
| 1 | 0 | 5 | 34.2 | 34.4 | 3 | 2 | 3 | 26.2 | 28.2 |
| 2 | 1 | 2 | 24.0 | 28.7 | 3 | 0 | 8 | 46.3 | 46.8 |
| 2 | 0 | 4 | 31.5 | 30.9 | 3 | 3 | 0 | 45.2 | 47.2 |
| 3 | 0 | 0 | 78.5 | 72.5 | | | | | |

* Overall isotropic temperature factor with $B = 0.8 \text{ \AA}^{-2}$ applied.

TABLE IV

BOND DISTANCES AND ANGLES FOR $\text{Ba}_{5/6}\text{Sr}_{1/6}\text{RuO}_3^a$

| Atoms | Distances, A | Angle, deg |
|--------------------------------------|--------------|------------|
| $\text{Ru}_1\text{-Ru}_2$ | 2.473 | |
| $\text{O}_1\text{-Ru}_2\text{-O}_2$ | 2.01 2.01 | 86 |
| $\text{O}_3\text{-Ru}_2\text{-O}_2$ | 2.00 2.01 | 91 |
| $\text{O}_3\text{-Ru}_2\text{-O}_1$ | 2.00 2.00 | 91 |
| $\text{O}_2\text{-Ba}^b\text{-O}_3$ | 2.85 | 58 |
| $\text{O}_3\text{-Ba}^b\text{-O}_8$ | 2.85 | 60 |
| $\text{Ru}_2\text{-O}_2\text{-Ru}_1$ | 2.00 | 76 |

^a The standard error in the Ru-Ru distance is about 0.03 A. The standard errors in the cat on-oxygen distances are in the range 0.03-0.05 A. Estimated standard errors in the angles are about 2° . ^b Ba = $\text{Ba}_{5/6}\text{Sr}_{1/6}$.

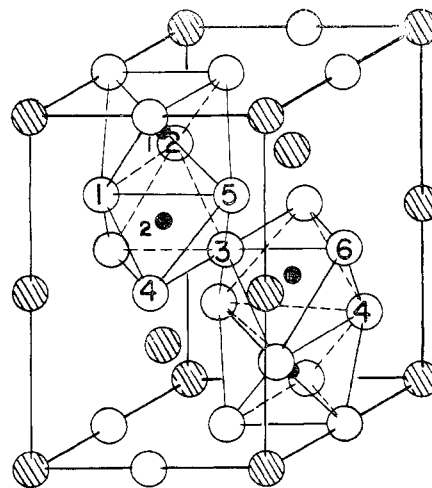


Figure 1.—Four-layer structure. This structure, previously reported for high-temperature BaMnO_3 , is adopted by $\text{Ba}_{5/6}\text{Sr}_{1/6}\text{RuO}_3$: ●, Ru; ○, O; ⊗, Ba, Sr.

be indexed on the basis of a hexagonal unit cell ($a = 5.76 \pm 0.01 \text{ A}$, $c = 22.2 \pm 0.1 \text{ A}$), but there were a number of reflections which could not be so indexed.

Single crystals were obtained as before from a barium chloride flux. The $h0l$ net obtained using a Buerger precession camera was very similar to that of BaRuO_3 but contained a number of weaker reflections which required a c axis of 44.4 A. The $h\bar{k}0$ net showed sixfold symmetry in the positions of reflections but not quite sixfold in their intensities. The true symmetry is therefore lower than hexagonal, and the pseudo-hexagonal cell has a c axis twice as long as that of BaRuO_3 .

In order to determine the extent to which BaIrO_3 resembles BaRuO_3 , about 50 $h0l$ superlattice reflections were ignored, and a least-squares refinement was carried out with the remaining

hkl data (91 reflections). The *R* factor dropped to 14.1%, showing the basic similarity between the two structures. However, the detailed structure of BaIrO₃ is not yet known.

Values of *x* from 1/6 to 5/6 in the system Ba_{1-x}Sr_xIrO₃ were tried. The phase with the four-layer structure was obtained pure at *x* = 1/3; its powder pattern could be indexed completely on the basis of a hexagonal unit cell with *a* = 5.707 ± 0.005 Å and *c* = 9.767 ± 0.005 Å. A refinement for this four-layer structure was carried out on the powder data. For this purpose, the Busing, Martin, and Levy least-squares program was adapted by Norman Morrow of our laboratory for the refinement of powder data including unresolved reflections. The *R* factor based on intensities dropped to 15.4% after four cycles. The final position parameters were: iridium *z* = 0.8866 ± 0.001 and oxygen *x* = 0.759 ± 0.015. The value of the oxygen parameter leads to an unreasonably close oxygen-oxygen distance for the three oxygen ions sharing the common face. This result and the experience with BaIrO₃ emphasize the need for further investigation of the oxygen positions (an investigation which is planned); however, the Ir-Ir distance is not likely to be affected very much and may be tentatively reported as 2.67 ± 0.03 Å in the four-layer structure. Table V lists the powder data.

TABLE V
X-RAY POWDER DATA FOR Ba_{2/3}Sr_{1/3}IrO₃

| H | K | L | DOBS | DCAL | IOBS | ICAL | H | K | L | DOBS | DCAL | IOBS | ICAL |
|---|---|---|-------|-------|-------|-------|---|---|---|-------|-------|------|------|
| 1 | 0 | 0 | 4.960 | 4.962 | 26.6 | 42.9 | 2 | 0 | 5 | 1.427 | 1.427 | 8.5 | 6.5 |
| 1 | 0 | 1 | 4.425 | 4.410 | 27.8 | 50.7 | 2 | 1 | 4 | 1.482 | 1.484 | 9.3 | 11.8 |
| 1 | 0 | 2 | 3.479 | 3.474 | 26.8 | 31.4 | 2 | 2 | 0 | 1.427 | 1.427 | 16.6 | 17.4 |
| 1 | 1 | 0 | 2.856 | 2.853 | 164.0 | 151.0 | 1 | 1 | 6 | 1.412 | 1.414 | 8.9 | 2.6 |
| 1 | 0 | 3 | 2.719 | 2.719 | 83.6 | 85.6 | 2 | 2 | 1 | | 1.412 | | |
| 2 | 0 | 0 | 2.465 | 2.471 | 7.0 | 2.6 | 3 | 0 | 4 | | 1.366 | | |
| 0 | 0 | 4 | 2.398 | 2.396 | 6.5 | 5.1 | 2 | 1 | 6 | 1.359 | 1.359 | | |
| 2 | 0 | 1 | 2.202 | 2.205 | 39.4 | 34.0 | 1 | 1 | 1 | 1.350 | 1.350 | 22.3 | 17.7 |
| 2 | 0 | 2 | 2.202 | 2.205 | 39.4 | 34.0 | 2 | 1 | 5 | 1.350 | 1.350 | | |
| 1 | 0 | 4 | 2.189 | 2.189 | | | 1 | 0 | 7 | 1.344 | 1.343 | | |
| 2 | 0 | 3 | 1.968 | 1.968 | 42.9 | 39.8 | 3 | 1 | 2 | 1.320 | 1.320 | 5.7 | 2.7 |
| 2 | 1 | 0 | 1.867 | 1.868 | 2.5 | 3.5 | 3 | 1 | 3 | 1.261 | 1.263 | 16.3 | 15.9 |
| 1 | 1 | 4 | 1.853 | 1.855 | 5.3 | 3.7 | 2 | 1 | 6 | 1.226 | 1.227 | | |
| 2 | 1 | 1 | 1.835 | 1.835 | 5.2 | 5.0 | 4 | 0 | 1 | 1.226 | 1.226 | 16.3 | 17.9 |
| 1 | 0 | 5 | 1.817 | 1.817 | 9.5 | 9.2 | 0 | 0 | 8 | 1.219 | 1.221 | | |
| 2 | 1 | 2 | 1.744 | 1.745 | 17.3 | 17.4 | 2 | 0 | 7 | 1.211 | 1.215 | | |
| 2 | 0 | 4 | 1.734 | 1.737 | | | 4 | 0 | 3 | 1.153 | 1.155 | 7.0 | 5.7 |
| 2 | 0 | 0 | 1.647 | 1.647 | 26.9 | 25.2 | 3 | 2 | 1 | | 1.126 | | |
| 2 | 1 | 3 | 1.620 | 1.620 | 42.7 | 39.0 | 1 | 1 | 8 | 1.121 | 1.122 | 15.2 | 15.3 |
| 1 | 0 | 6 | 1.544 | 1.546 | 6.84 | 7.5 | 3 | 1 | 5 | | 1.122 | | |

The distorted perovskite phase similar to the corresponding ruthenium compound was obtained at *x* = 2/3. At *x* = 5/6 the perovskite phase was present along with another unidentified phase, the pattern of which resembled that of Sr₂IrO₄.

Discussion

If we assume that the oxygen octahedra formed by the close-packed AO₃ layers are regular, the distance between centers of the face-sharing octahedra is 2.37 Å in the phase of composition Ba_{5/6}Sr_{1/6}RuO₃. The Ru-Ru distance of 2.47 Å shows the effect of repulsive forces between the Ru⁴⁺ cations. For the high-temperature form of BaMnO₃, the distance between centers of face-shared octahedra is 2.34 Å while the Mn-Mn distance is reported as 2.62 Å. One might conclude that there are stronger bonds between the Ru⁴⁺ ions than the Mn⁴⁺ ions. However, the large error possible in the Mn-Mn distance makes any such conclusion highly tentative.

In the nine-layer structure of BaRuO₃, the Ru-Ru distance is 2.55 Å while the distance between centers of face-sharing octahedra is 2.40 Å. The larger Ru-Ru distance might be due to a weaker metal-metal interaction when the central ion has to form two bonds.

The range of *x* in the different phases of the system Ba_{1-x}Sr_xRuO₃ could not be determined since it was obvious that equilibrium was not reached. Cell

volumes were found to change with changing strontium content in products containing the same two phases. Even repeated grinding and heating failed to give concordant results. Higher temperatures appeared to favor the conversion from the nine-layer to the four-layer structure. Thus, with *x* = 0.05, only the nine-layer structure was found at 1000°, but at 1100°, both the nine-layer and four-layer structures were found. With *x* = 0.1, only the nine-layer structure was present in the product at 1000°, and only the four-layer structure was in the product at 1100°. Upon increasing *x* to 0.15, none of the products at any temperature gave the nine-layer structure. We might place the upper limit at *x* = 0.1 for the nine-layer structure, but this value might be increased considerably if low-temperature methods of synthesis such as hydrothermal methods could be employed. The four-layer structure is clearly the stable phase in the temperature range 1100–1200° with *x* = 0.10 and in the temperature range 1000–1200° when 0.15 ≤ *x* ≤ 0.2. The lattice dimensions are *a* = 5.717 ± 0.005 Å, *c* = 9.49 ± 0.01 Å when *x* = 0.1 and *a* = 5.706 ± 0.005 Å, *c* = 9.485 ± 0.01 Å when *x* = 0.20. The perovskite phase makes its appearance in the products when 0.25 ≤ *x* ≤ 0.35. The lattice dimensions for the four-layer structure vary in these products from *a* = 5.700 ± 0.005 Å, *c* = 9.481 ± 0.01 Å, *x* = 0.25 at 1000° to *a* = 5.692 ± 0.005 Å, *c* = 9.473 ± 0.01 Å, *x* = 0.35 at 1200°. Only the perovskite phase was found in mixtures with *x* ≥ 0.5.

It should be noted that, over the range of composition of the four-layer structure, the *a* axis decreases more sharply than the *c* axis with increasing strontium content. This could be due to the repulsive forces between the pairs of Ru⁴⁺ ions in the face-shared octahedra. The system Ba_{1-x}Sr_xIrO₃ is different in some important respects from the ruthenium system in that the end members are different. The larger unit cell required at *x* = 0 and the indications obtained from the variations of the temperature factors for the oxygens suggest that the structure contains ordered oxygen vacancies. The structure, however, is closely related to that of the nine-layer ruthenium compound. It takes appreciably more strontium (*x* ≥ 0.33) to give the four-layer structure, and the transformation does not appear to be so sensitive to temperature changes in the range studied. No evidence of a superlattice was obtained with the four-layer structure. With larger proportions of strontium, an orthorhombic perovskite phase is formed. Thus, in general, the two systems behave in a similar manner.

The end member in the iridium system (*x* = 1) has not been made. Randall⁴ found that all attempts to prepare SrIrO₃ led invariably to Sr₂IrO₄, with the K₂NiF₄ structure. The perovskite-type phase could be obtained in the system SrRu_{1-x}Ir_xO₃ up to *x* = 0.5. It is interesting that substitution of Ba for one-third of the Sr will stabilize the perovskite phase.

There is an inherent difficulty in studying these systems by solid-state reactions. Because of the topo-

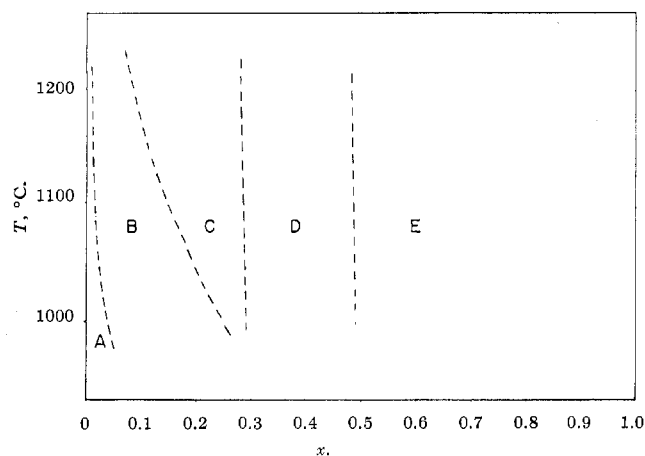


Figure 2.—The system $\text{Ba}_{1-x}\text{Sr}_x\text{RuO}_3$: A, nine-layer-structure-type region; B, two-phase region, nine-layer and four-layer types; C, four-layer-structure-type region; D, two-phase region, four-layer and perovskite types; E, perovskite-structure-type region.

chemical nature of the reactions, local concentration of reactants inevitably must vary. Conditions are far from equilibrium. The products are phases of high lattice energy in which diffusion of ions is slow at the temperatures used in these experiments. This is probably the reason for the observed variability in the cell dimensions of phases in two-phase regions. Structure data for the system $\text{Ba}_{1-x}\text{Sr}_x\text{RuO}_3$ are summarized in Figure 2.

Figure 3 is a highly tentative description of the system $\text{Ba}_{1-x}\text{Sr}_x\text{Ru}_{1-y}\text{Ir}_y\text{O}_3$ based on the data for about 1000° . For the purpose of this description the upper right-hand corner of the figure has been labeled " SrIrO_3 ." This section of the diagram is indicated by dotted lines. SrIrO_3 , as mentioned earlier, is still hypothetical; previous attempts to make it produced Sr_2IrO_4 .

The thickness of the AO_3 layer is shown to be an important factor in the stacking sequence of the layers.

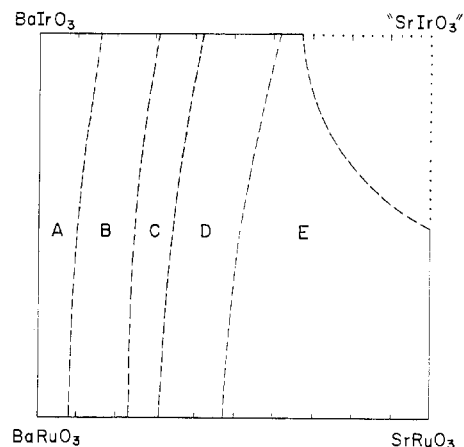


Figure 3.—Tentative description of the system $\text{Ba}_{1-x}\text{Sr}_x\text{Ru}_{1-y}\text{Ir}_y\text{O}_3$ at about 1000° : A, nine-layer-structure-type region; B, two-phase region, nine-layer and four-layer types; C, four-layer-structure-type region; D, two-phase region, four-layer and perovskite types; E, perovskite-type region. The area near the " SrIrO_3 " corner is the unrealized portion of the perovskite-type region.

If metal-metal bonding plays a part in bringing about hexagonal close packing of the layers, the repulsive forces also seem to be significant. When the decrease in layer thickness would bring the M cations too close together, the stacking sequence tends to become cubic and the M cations are separated by an oxide ion; *i.e.*, the coordination polyhedra share corners rather than faces.

Acknowledgments.—Part of this work was supported by the National Science Foundation under Grant GP-1396. Computations were carried out in the Computer Center of the University of Connecticut, which is supported in part by Grant GP-1819 of the National Science Foundation. Assistance of National Science Foundation Grant GP-3461 is also acknowledged. The authors thank Mr. Norman Morrow for adapting the Busing, Martin, and Levy least-squares refinement program for powder intensity work.